

## Evaluation of $y(\text{HM}_{1402015})$ with respect to NICT-Sr1 for the period MJD 58644 to 58679

The frequency of hydrogen maser  $\text{HM}_{1402015}$  was evaluated for the period from MJD 58644 to 58679 (June 10 – July 15 in 2019) using secondary frequency standard NICT-Sr1. In terms of the fractional deviation from the nominal frequency, we find  $\overline{y(\text{HM}_{1402015})} = -9.61347 \times 10^{-13}$ . The optical lattice clock acquired data for 697,444 s (23.1% of the total evaluation period) during three operating intervals on MJD 58646, 58658 to 58666 and 58675 as shown in Fig. 1. The resulting uncertainties are represented in the following table according to Circular T notation:

Period of Estimation (MJD)	$\overline{y(\text{HM}_{1402015})}$	$u_A$	$u_B$	$u_{l/\text{Lab}}$	$u_{\text{Srep}}$
58644 – 58679	-9613.47	0.08	0.71	2.08	4
Effect	Uncertainty	$u_A$	$u_B$	$u_A$	$u_B$
$u_{A/\text{Sr}}$	0.08	✓			
$u_B$	0.71		✓		
HM: linear trend estimation	0.48			✓	
HM: stochastic noise	2.02			✓	
Optical-microwave comparison / microwave transfer	0.14				✓
Uncertainty of Sr as SRS	4				✓

Table 1. Results of evaluation. All number are in parts of  $10^{-16}$ .

The evaluation employs the recommended value of the  $^{87}\text{Sr}$  clock transition as a secondary representation of the definition of the second:  $\nu(^{87}\text{Sr}) = 429\,228\,004\,229\,873.0$  Hz with its relative standard uncertainty of  $u_{\text{Srep}} = 4 \times 10^{-16}$ , determined by the 21<sup>st</sup> CCTF in June 2017.

$u_A$  is the Type A uncertainty of NICT-Sr1 as an optical standard. It represents the statistical uncertainty determined by interleaved measurements [1].

$u_B$  is the Type B uncertainty of NICT-Sr1 [1 – 3], including the uncertainty of the gravitational redshift.

$u_{l/\text{Lab}} = 2.08 \times 10^{-16}$  is the uncertainty due to the link between NICT-Sr1 and the HM [2, 3]. It consists of the Type B uncertainty  $u_{B,l/\text{Lab}} = 1.4 \times 10^{-17}$  due to the frequency comparison between microwave and optical signals, including distribution of the microwave signals, and the Type A uncertainty  $u_{A,l/\text{Lab}} = 2.07 \times 10^{-16}$  representing the linear trend estimation of the HM ( $u_{l/\text{trend}}$ ) and the additional uncertainty due to the stochastic noise of the HM during unobserved intervals ( $u_{l/\text{stoch}}$ ).

### 1. Evaluation of the frequency of hydrogen maser $\text{HM}_{1402015}$ with respect to NICT-Sr1 over 35 days

The  $^{87}\text{Sr}$  optical lattice clock NICT-Sr1 was operated in the same mode during all operating intervals. The details of NICT-Sr1 are described in [1, 2]. The Sr atoms were laser-cooled using a two-stage laser cooling technique and loaded to a vertically oriented one-dimensional optical

lattice. The optical frequency at the wavelength of 698 nm stabilized to NICT-Sr1 was down-converted to a microwave frequency using an Yb: fiber-based frequency comb. By stabilizing the comb to the optical reference with appropriately chosen frequency offsets, an optically generated microwave with a frequency of 9.25 GHz was derived from the thirty-seventh harmonic of the repetition rate (= 250 MHz), assuming an optical frequency of the clock transition according to the recommended value as a secondary representation of the definition of the second  $\nu(^{87}\text{Sr})$ . The microwave frequency was then down-mixed to 50 MHz using a 9.2 GHz signal provided by an oscillator phase-locked to the 100 MHz signal of HM<sub>1402015</sub>. The down-mixed signal was counted and recorded every second by a zero-dead-time frequency counter referenced to the same HM.

The fractional deviation of the HM frequency from its nominal value is stored pre-averaged in 10 s bins. To assign appropriate weights, a statistical uncertainty determined from a daily stability estimate and the number of contributing datapoints is also stored for each bin.

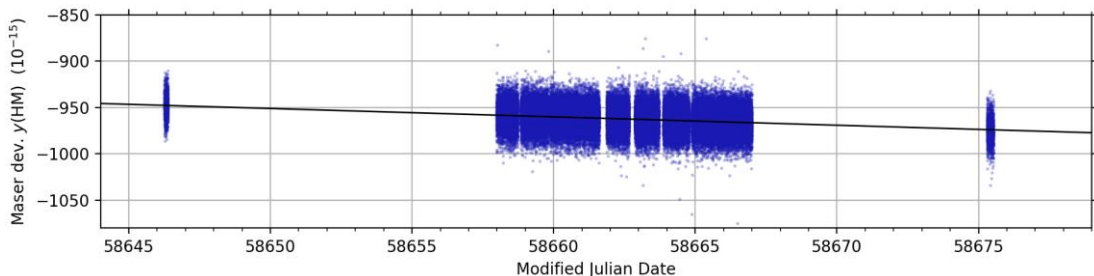


Fig. 1. Distribution of maser frequency measurements in terms of fractional deviation  $y(\text{HM})$  from the nominal frequency. Displayed data has been corrected for deviations from nonlinear drift determined through comparison to the HM ensemble. Black solid line indicates the linear fit used for drift removal.

## 2. Treatment of stochastic noise during unobserved intervals

For intermittent clock operation, phase and frequency excursions of the HM during unobserved intervals contribute significant measurement uncertainty [2].

To mitigate their overall effect, we include a total of three HMs in the evaluation (HM<sub>1402004</sub>, HM<sub>1402014</sub> and HM<sub>1402015</sub>). Their relative phase is continuously monitored by the dual-mixer time difference (DMTD) system used in the generation of Japan Standard Time. We calculate the phase difference of each HM from the ensemble average phase and confirm the absence of abnormal behavior during the evaluation period. We then determine the frequency of HM<sub>1402015</sub> with respect to the ensemble. By subtracting frequency offset and linear trend from this relative frequency, we obtain residuals that approximate the instantaneous deviation of HM<sub>1402015</sub> from a pure linear drift, while summing to zero over the evaluation period. We use these residuals (calculated for a set of one-hour intervals) to correct the HM frequency measured with respect to the Sr clock. The result is an improved representation of the mean frequency and linear drift of HM<sub>1402015</sub> over the complete evaluation period. A weighted linear fit is applied to the corrected data to find the frequency corresponding to the midpoint of the 35-day interval.

We characterize the typical instability of a single maser based on evaluation of several years of continuous data using three-corner-hat methods, and find that for large averaging times it is well-described by an Hadamard variance  $\sigma_{\text{H}}^2(\tau) = a_{-1} + a_{-3} \tau^2$ . Here,  $a_{-1} = (2.2 \times 10^{-16})^2$  represents flicker frequency noise (FFN) [4] while the slow-varying noise that dominates the long-term instability through  $a_{-3} = (3.4 \times 10^{-22}/\text{s})^2$  is referred to as flicker-walk frequency modulation (FWFM) [5]. We follow the approach described in the supplement of ref. [6] to determine the uncertainty of extrapolating from the inhomogeneously distributed data to the full evaluation

period. This yields a distribution-specific sensitivity to the HM's noise power spectral densities (PSD) [6], which we obtain from the observed maser instabilities  $a_{-1}$  and  $a_{-3}$  through the relations

$$\text{FFN: } \sigma_{\text{H}}^2(\tau) = \frac{1}{2} \ln\left(\frac{256}{27}\right) h_{-1} \quad \text{for } S_y^{\text{FFN}} = h_{-1} f^{-1} \quad \text{and} \quad (1)$$

$$\text{FWFM: } \sigma_{\text{H}}^2(\tau) = \frac{16}{6} \pi \ln\left(\frac{3}{4} \cdot 3^{11/16}\right) h_{-3} \tau^2 \quad \text{for } S_y^{\text{FWFM}} = h_{-3} f^{-3} \quad , \quad (2)$$

according to ref. [5, 7]. Despite the complexity of FFN and FWFM in the temporal domain, the noise can always be expressed as a sum over normally distributed sources, and there is no correlation between the noise encountered in separate masers. The maser ensemble therefore shows the same uncertainty reduction with  $N_{\text{ens}}^{-1/2}$  as other noise types.

For the present (inhomogeneous) measurement distribution and PSDs, this leads to the uncertainty contributions  $u_{1/\text{FFN}} = 1.11 \times 10^{-16}$  and  $u_{1/\text{FWFM}} = 1.68 \times 10^{-16}$ , which we include as  $u_{1/\text{stoch}} = 2.02 \times 10^{-16}$ .

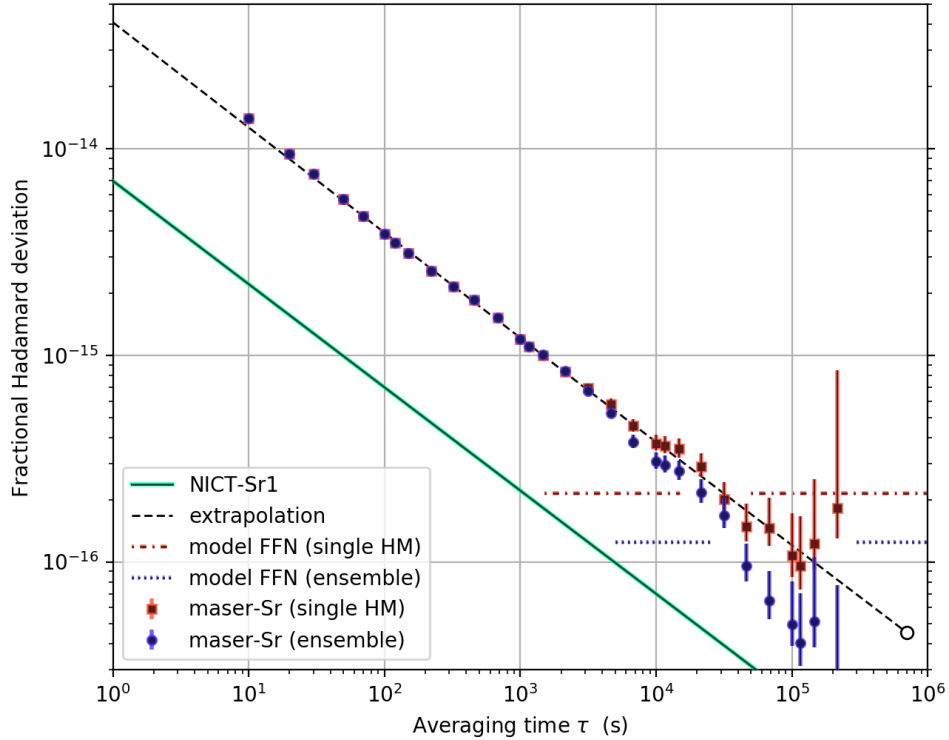


Fig.2. Instability of maser frequency measurements with respect to Sr. Blue circles and red squares show the overlapping Hadamard deviation for the residuals from a linear fit with and without correction for deviation from linear drift of the HM, as determined using an ensemble of 3 HMs. Gaps have been removed by contracting the data into a continuous interval. Error bars indicate  $1\sigma$  uncertainties, calculated for white frequency noise. The dashed line indicates the extrapolation to the full length of available data, used to obtain the statistical uncertainty. For long averaging times, the Hadamard deviation falls to a level consistent with the flicker noise floor of the maser stability model, indicated by the dot-dashed line for a single maser, and by the dotted line for the ensemble, where the instability is expected to improve by a factor of  $1/\sqrt{N_{\text{ens}}}$ . The green line shows the instability contribution from NICT-Sr1.

### 3. Determination of statistical and systematic contributions to $u_{l/\text{Lab}}$

We determine a statistical uncertainty of the maser frequency measurement  $u_{\text{stat}} = 4.6 \times 10^{-17}$  from the residuals of a linear fit by extrapolating the Allan deviation from the region limited by white frequency noise (30-3000 s) to the full length of available data.

When plotting the instability of the frequency measurements for only HM<sub>1402015</sub> in terms of the Hadamard deviation, we expect an observed flicker floor  $\sigma_L^2 \approx a_{-1}$  due to FFN. After applying corrections for nonlinear drift, the results represent the stability of the entire ensemble used to determine the corrections. As shown in Fig. 2, observations are indeed consistent with instabilities at or below  $\sigma_L \approx 2.2 \times 10^{-16}$  before correction, and  $\sigma_L/N_{\text{ens}}^{1/2} \approx 1.2 \times 10^{-16}$  afterwards.

Since the midpoint (MJD 58661.5) of the evaluation period differs from the barycenter of the data by 89,428 s, the uncertainty of the maser drift rate contributes an uncertainty of  $u_{\text{drift}} = 1.5 \times 10^{-17}$ , such that  $u_{l/\text{trend}} = (u_{\text{stat}}^2 + u_{\text{drift}}^2)^{1/2} = 4.8 \times 10^{-17}$ .

While intermittent measurements of the maser frequency are easily affected by phase shifts resulting from thermalization effects at the start of frequency comb operation, as well as from diurnal temperature variation, an investigation of data obtained over a ten-day interval [8] sets a limit of  $u_{B,l/\text{Lab}}^{\text{typ}} = 7.95 \times 10^{-17}$  for the window of  $T_{\text{typ}} = 6$  h duration during which intermittent measurements are typically performed. We assign this uncertainty to the shorter measurements on MJD 58646 and 58675.

During this evaluation, most of the data was obtained during a near-continuous measurement spanning  $T_{\text{ext}} = 216$  h. For such an extended interval, phase excursions of similar magnitude result in a reduced uncertainty

$$u_{B,l/\text{Lab}}^{\text{ext}} = u_{B,l/\text{Lab}}^{\text{typ}} \cdot (T_{\text{typ}}/T_{\text{ext}}) = 2.2 \times 10^{-18}.$$

We determine a combined systematic uncertainty  $u_{B,l/\text{Lab}} = 1.4 \times 10^{-17}$  from a weighted mean over the variances  $(u^2)_{B,l/\text{Lab}}^{\text{typ}}$  and  $(u^2)_{B,l/\text{Lab}}^{\text{ext}}$ . The near-continuous measurements from MJD 58658 to 58666 contribute 97% of the data and are weighted accordingly.

## 4. Accuracy of NICT-Sr1

The systematic corrections and their uncertainties for NICT-Sr1 [1 – 3] are summarized below:

Effect	Correction ( $10^{-17}$ )	Uncertainty ( $10^{-17}$ )
Blackbody radiation	513.1	3.4
Lattice scalar / tensor	0	5.3
Lattice hyperpolarizability	-0.2	0.1
Lattice E2/M1	0	0.5
Probe light	0.1	0.1
Dc Stark	0.1	0.2
Quadratic Zeeman	51.2	0.3
Density	0.4	0.9
Background gas collisions	0	1.8
Line pulling	0	0.1
Servo error	1.8	1.5
Total	566.6	6.8
Gravitational redshift	-834.1	2.2
Total (with gravitational effect)	-267.5	7.1

Table 2. Systematic corrections and their uncertainties for NICT-Sr1.

## 5. References

- [1] H. Hachisu and T. Ido, “Intermittent optical frequency measurements to reduce the dead time uncertainty of frequency link,” *Jpn. J. Appl. Phys.* **54**, 112401 (2015).
- [2] H. Hachisu, G. Petit, F. Nakagawa, Y. Hanado and T. Ido, “SI-traceable measurement of an optical frequency at low  $10^{-16}$  level without a local primary standard,” *Opt. Express* **25**, 8511 (2017).
- [3] H. Hachisu, F. Nakagawa, Y. Hanado and T. Ido, “Months-long real-time generation of a time scale based on an optical clock,” *Sci. Reports* **8**, 4243 (2018).
- [4] D. Allan, “Time and frequency (time-domain) characterization, estimation, and prediction of precision clock and oscillators,” *IEEE UFFC* **34**, 647 (1987).
- [5] W. J. Riley, “Handbook of Frequency Stability Analysis,” NIST Special Publication 1065 (2008)
- [6] C. Grebing *et al.*, “Realization of a timescale with an accurate optical lattice clock,” *Optica* **3**, 563-569 (2016).
- [7] S.T. Dawkins, J. J. McFerran and A. Luiten, “Considerations on the Measurement of the Stability of Oscillators with Frequency Counters”, *IEEE Trans. UFFC* **54**, 918-925 (2006).
- [8] Evaluation report “nict-sr1\_58454-58464 [January 2019]”, available at <https://www.bipm.org/en/bipm-services/timescales/time-ftp/data.html>.